

Spark Deficient Gabor Frame Provides a Novel Analysis Operator for Compressed Sensing

Vasiliki Kouni^{1,2} and Holger Rauhut¹

¹ Chair for Mathematics of Information Processing, RWTH Aachen University,
Aachen, Germany

`kouni@mathc.rwth-aachen.de`, `rauhut@mathc.rwth-aachen.de`

² Department of Informatics and Telecommunications, National and Kapodistrian
University of Athens, Athens, Greece
`vicky-kouni@di.uoa.gr`

Abstract. The analysis sparsity model is a very effective approach in modern Compressed Sensing applications. Specifically, redundant analysis operators can lead to fewer measurements needed for reconstruction when employing the analysis l_1 -minimization in Compressed Sensing. In this paper, we pick an eigenvector of the Zauner unitary matrix and –under certain assumptions on the ambient dimension– we build a spark deficient Gabor frame. The analysis operator associated with such a spark deficient Gabor frame, is a new (highly) redundant Gabor transform, which we use as a sparsifying transform in Compressed Sensing. We conduct computational experiments –on both synthetic and real-world data– solving the analysis l_1 -minimization problem of Compressed Sensing, with four different choices of analysis operators, including our Gabor analysis operator. The results show that our proposed redundant Gabor transform outperforms –in all cases– Gabor transforms generated by state-of-the-art window vectors of time-frequency analysis.

Keywords: Compressed Sensing · analysis sparsity · Gabor transform · window vector · spark deficient Gabor frame.

1 Introduction

Compressed Sensing (CS) [1] is a modern technique to recover vectors $x \in \mathbb{V}^L$ ($\mathbb{V} = \mathbb{R}$ or \mathbb{C}) from few linear and possibly corrupted measurements

$$y = Ax + e \in \mathbb{V}^K \quad (1)$$

with $K < L$. The applications of CS vary from Radar Imaging [2], Cryptography [3] and Telecommunications [4], to Magnetic Resonance Imaging (MRI) [5], Deep Learning [6] and Computer Graphics [7].

1.1 Related Work

CS heavily relies on sparsity/compressibility of the signal of interest x . A signal x is called *s-sparse* if it has at most s nonzero entries, while it is called

compressible if it is well approximated by an s -sparse vector. Sparsity models are split in two categories: synthesis sparsity and analysis sparsity. Synthesis sparsity model [8] is by now very well studied [9], [10], [11], [12]. On the other hand, significant research has also been conducted over the last years towards its analysis counterpart [13], [14], [15], [16], (also known as co-sparse model [17], [18]), due to the flexibility it provides in modelling sparse signals, since it leverages the redundancy of the involved analysis operators. Related work [14] has also demonstrated that it is computationally more appealing to solve the optimization algorithm of analysis CS since a) the actual optimization takes place in the ambient space b) the algorithm may need less measurements for perfect reconstruction, if one uses a redundant transform instead of an orthogonal³ one.

1.2 Motivation

In this work, we are motivated by results of [14], [17], [18] and [19]. These publications propose either analysis operators associated to redundant frames (i.e. matrices whose atoms/rows form a frame of the ambient space) with atoms in general position, or a finite difference operator (associated to the popular method of total variation [20]), in which many linear dependencies appear for large dimensions. In a similar spirit, in this paper we also deploy frames, but we differentiate our approach from the previous works by using *spark deficient frames*, i.e. their elements are not in general linear position. Our intuition behind employing spark deficient frames is based on remarks of [18]. According to the union-of-subspaces model [21], it is desired to have analysis operators that exhibit high linear dependencies among their rows and this is a condition satisfied by spark deficient frames. To that end, we introduce a novel analysis operator associated with a spark deficient Gabor frame (SDGF). Such a frame can be generated by time-frequency shifts of any eigenvector of the Zauner unitary matrix [22], under certain assumptions. To the best of our knowledge, its efficiency when combined with CS has not yet been demonstrated. Moreover, since Gabor transforms are little explored in terms of CS [12], [23], [24], we compare our proposed Gabor transform to three other Gabor transforms –serving as baseline– which emerge from state-of-the-art window vectors in time-frequency analysis. Finally, we illustrate the practical importance of our method not only for synthetic data, but for real-world signals too.

1.3 Key Contributions

Our novelty is twofold: (a) we generate a SDGF based on a window vector, associate this SDGF to a new Gabor analysis operator and use the latter as a sparsifying transform in analysis CS (b) we compare numerically our proposed method with three other Gabor analysis operators, based on common windows of time-frequency analysis, on both synthetic and real-world data. Our experiments

³ synthesis and analysis models coincide when the analysis operator is orthogonal/unitary

show that our method outperforms all others consistently for synthetic and real-world signals.

The rest of the paper is organized as follows: in Section II we give notation, briefly introduce the setup of CS and explain how we tailor it to our purpose. Section III describes Gabor frames and extends to spark deficient ones, building the desirable SDGF and its analysis operator. Section IV contains the results of our numerical experiments. Lastly, in Section V we make some concluding remarks and give potential future directions.

2 Compressed Sensing setup

2.1 Notation

- For a set of indices $N = \{0, 1, \dots, N-1\}$, we write $[N]$.
- (Bra-kets) The set of (column) vectors $|0\rangle, |1\rangle, \dots, |L-1\rangle$ is the standard basis of \mathbb{C}^L .
- We write \mathbb{Z}_L for the ring of residues mod L , that is $\mathbb{Z}_L = \{0 \bmod L, 1 \bmod L, \dots, (L-1) \bmod L\}$.
- We write $a \equiv b \pmod{L}$ for the congruence modulo, where $a, b \in \mathbb{Z}$.
- The support of a signal $x \in \mathbb{V}^L$ is denoted by $\text{supp}(x) = \{i \in [L] : x_i \neq 0\}$. For its cardinality we write $|\text{supp}(x)|$ and if $|\text{supp}(x)| \leq s \ll L$, we call x s -sparse.

2.2 Analysis Compressed Sensing Formulation

As already described in Section I, the main idea of CS is to reconstruct a signal $x \in \mathbb{V}^L$ from

$$y = Ax + e \in \mathbb{V}^K, \quad (2)$$

$K < L$, where A is the so-called measurement matrix and $e \in \mathbb{V}^K$, with $\|e\|_2 \leq \eta$, corresponds to noise. To do so, we first assume there exists a redundant sparsifying transform $\Phi \in \mathbb{V}^{P \times L}$ ($P > L$) called the analysis operator, such that Φx is (approximately) sparse.

On the other hand, the choice of A is tailored to the application for which CS is employed. For example, in MRI, A is a randomly subsampled Fourier matrix [5] or in duplex ultrasonography [25], A is a randomly subsampled identity operator. There exist conditions on A which ensure exact or approximate reconstruction of x , such as the *coherence* or the *restricted isometry property* [8]. A standard CS setup involves subsampling uniformly at random the rows of an isometry matrix $U \in \mathbb{V}^{L \times L}$ and it has proven to work well [9], since it meets the aforementioned conditions. Hence, we choose a randomly subsampled identity operator as the measurement matrix A for the rest of the paper.

Now, using analysis sparsity in CS, we wish to recover x from y , that is to solve the *analysis l_1 -minimization* problem

$$\min_{x \in \mathbb{V}^L} \|\Phi x\|_1 \quad \text{subject to} \quad \|Ax - y\|_2 \leq \eta, \quad (3)$$

or a regularized version [26] of it:

$$\min_{x \in \mathbb{V}^L} \|\Phi x\|_1 + \frac{\mu}{2} \|x - x_0\|_2^2 \quad \text{subject to} \quad \|Ax - y\|_2 \leq \eta, \quad (4)$$

where x_0 denotes an initial guess on x and $\mu > 0$ is a smoothing parameter⁴.

We will devote the next Section to the construction of a suitable analysis transform Φ .

3 Gabor Frames

3.1 Gabor Systems

A *discrete Gabor system* (g, a, b) [27] is defined as a collection of time-frequency shifts of the so-called window vector $g \in \mathbb{C}^L$, expressed as

$$g_{n,m}(l) = e^{2\pi i m b l / L} g(l - na), \quad l \in [L], \quad (5)$$

where a, b denote time and frequency parameters (lattice parameters) respectively, $n \in [N]$ chosen such that $N = L/a \in \mathbb{N}$ and $m \in [M]$ chosen such that $M = L/b \in \mathbb{N}$ denote time and frequency shift indices respectively. If (5) spans \mathbb{C}^L , it is called *Gabor frame* and an equivalent definition of a frame [28] is given below.

Definition 1. Let $L \in \mathbb{N}$ and $(\phi_p)_{p \in P}$ a finite subset of \mathbb{C}^L . If the inequalities

$$c_1 \|x\|_2^2 \leq \sum_{p \in P} |\langle x, \phi_p \rangle|^2 \leq c_2 \|x\|_2^2 \quad (6)$$

hold true for all $x \in \mathbb{C}^L$, for some $0 < c_1 \leq c_2$ (frame bounds), then $(\phi_p)_{p \in P}$ is called a *frame* for \mathbb{C}^L .

The number of elements in (g, a, b) according to (5) is $P = MN = L^2/ab$ and if (g, a, b) is a frame, we have $ab < L$ (we shall refer to this situation from now on as oversampling [29]). A crucial ingredient in order to have good time-frequency resolution of a signal with respect to a Gabor frame, is the appropriate choice of the time-frequency parameters a and b . Apparently, this challenge can only be treated by numerically experimenting with different choices of a, b with respect to L .

Now, we associate to the Gabor frame (g, a, b) the following operator.

Definition 2. Let $\Phi_g : \mathbb{C}^L \mapsto \mathbb{C}^{M \times N}$ denote the Gabor analysis operator –also known as digital Gabor transform⁵ (DGT)– whose action on a signal $x \in \mathbb{C}^L$ is defined as

$$c_{m,n} = \sum_{l=0}^{L-1} x_l \overline{g(l - na)} e^{-2\pi i m b l / L}, \quad (7)$$

for $m \in [M], n \in [N]$.

⁴ in terms of optimization, it is preferred to solve (4) instead of (3)

⁵ so we will interchangeably use both terms from now on

3.2 Spark Deficient Gabor Frames

Let us first introduce some basic notions needed in this subsection.

Definition 3. *The symplectic group $\text{SL}(2, \mathbb{Z}_L)$ consists of all matrices*

$$G = \begin{pmatrix} \alpha & \beta \\ \gamma & \delta \end{pmatrix} \quad (8)$$

such that $\alpha, \beta, \gamma, \delta \in \mathbb{Z}_L$ and $\alpha\delta - \beta\gamma \equiv 1 \pmod{L}$. To each such matrix corresponds a unitary matrix given by the explicit formula [30]

$$U_G = \frac{e^{i\theta}}{\sqrt{L}} \sum_{u,v=0}^{L-1} \tau^{\beta^{-1}(\alpha v^2 - 2uv + \delta u^2)} |u\rangle \langle v|, \quad (9)$$

where θ is an arbitrary phase, β^{-1} is the inverse⁶ of $\beta \pmod{L}$ and $\tau = -e^{\frac{i\pi}{L}}$.

Definition 4. *The spark of a set F —denoted by $\text{sp}(F)$ —of P vectors in \mathbb{C}^L is the size of the smallest linearly dependent subset of F . A frame F is full spark if and only if every set of L elements of F is a basis, or equivalently $\text{sp}(F) = L+1$, otherwise it is spark deficient.*

Based on the previous definition, a Gabor frame with $P = L^2/ab$ elements of the form (5) is full spark, if and only if every set of L of its elements is a basis. Now, as proven in [28], almost all window vectors generate full spark Gabor frames, so the SDGFs are generated by exceptional window vectors. Indeed, the following theorem was proven in [30] and informally stated in [31], for the Zauner matrix $\mathcal{Z} \in \text{SL}(2, \mathbb{Z}_L)$ given by

$$\mathcal{Z} = \begin{pmatrix} 0 & -1 \\ 1 & -1 \end{pmatrix} \equiv \begin{pmatrix} 0 & L-1 \\ 1 & L-1 \end{pmatrix}. \quad (10)$$

Theorem 1 ([30]). *Let $L \in \mathbb{Z}$ such that $2 \nmid L$, $3 \mid L$ and L is square-free. Then, any eigenvector of the Zauner unitary matrix $U_{\mathcal{Z}}$ (produced by combining (9) and (10)), generates a spark deficient Gabor frames for \mathbb{C}^L .*

Therefore, in order to produce a SDGF and apply its associated analysis operator in CS, we must first choose an ambient dimension L that fits the assumptions of Theorem 1. Then, we calculate $U_{\mathcal{Z}}$ using (9) and (10) and in the end, perform its spectral decomposition in order to acquire its eigenvectors. Since all the eigenvectors of $U_{\mathcal{Z}}$ generate SDGFs, we may choose without loss of generality an arbitrary one, which we call *star window* and denote it as g_* from now on. We call the analysis operator associated with such a SDGF *star DGT* and denote it Φ_{g_*} , in order to indicate the dependance on g_* . We coin the term "star", due to the slight resemblance of this DGT to a star when plotted in Matlab.

⁶ $bb^{-1} \equiv 1 \pmod{L}$

Remark 1. A simple way to choose L , is by considering its prime factorization: take k prime numbers $p_1^{\alpha_1}, p_2^{\alpha_2}, \dots, p_k^{\alpha_k}$, with $p_1 = 3$ and $\alpha_1, \alpha_2, \dots, \alpha_k$ not all a multiple of 2, such that $L = 3^{\alpha_1} p_2^{\alpha_2} \dots p_k^{\alpha_k}$. Since $a, b \mid L$, we may also choose a, b to be one, or a multiplication of more than one, prime numbers from the prime factorization of L . We have seen empirically that this method for fixing (L, a, b) produces satisfying results, as it is illustrated in the figures of the upcoming pages.

4 Numerical Experiments

4.1 Signals' description

We run experiments on 4 synthetic data and 6 real-world speech signals, taken from Wavelab package [32] and TIMIT corpus [33] respectively. All signals are real-valued; the real-world data are sampled at 16 kHz. Since not each signal's true dimension matches the conditions imposed by Theorem 1, we cut-off each signal to a specific ambient dimension L being as closer as it gets to its true dimension, in order to capture a meaningful part of the signal. For each of the signals, we follow almost the same procedure with minor adaptations, presented in the next subsection.

4.2 Proposed framework

The steps of our method are now summarized below.

1. For the real-world signals: we fix each ambient dimension L to match the conditions of Theorem 1, using also Remark 1, so that the constructed L is as closer as it gets to the true ambient dimension. After that, we set the time-frequency parameters (a, b) accordingly, to provide good time-frequency representation of each signal, then load the signal and cut it off to the first L entries. We consider a row vector K of 1000 evenly spaced points between 1 and L and use it as the measurements' interval.
2. For the synthetic signals: we construct as previously each ambient dimension L and directly initialize each signal according to this choice of L . We vary the number of measurements K in the range $\{1, 2, \dots, L\}$.
3. We use the power iteration method [34] which yields the largest in magnitude eigenvalue and corresponding eigenvector of U_Z , then set this eigenvector as our desired window vector g_* .
4. For each signal, we generate –using the MATLAB package *LTFAT* [35]– four different Gabor frames with their associated analysis operators/DGTs, which go as follows: Φ_{g_1} , Φ_{g_2} , Φ_{g_3} and Φ_{g_*} , corresponding to a Gaussian, a Hann, a Hamming [27] and the star window vector respectively. Since we process real-valued signals, we alter the four analysis operators to compute only the DGT coefficients of positive frequencies instead of the full DGT coefficients.
5. For each choice of K in the measurements' interval:

- we set up a randomly subsampled identity operator $A \in \mathbb{R}^{K \times L}$, determine the measurement vector

$$y = Ax \quad (11)$$

and add to y Gaussian noise e with zero mean and standard deviation $\sigma = 0.001$,

- we solve –using the MATLAB package *TFOCS* [26]– four different instances of (4), one for each of the four DGTs. For TFOCS, we use the *solver_BPDN_W* solver, set $x_0 = A^T Ax$ or $x_0 = 0$, $z_0 = []$ and $\text{opts} = []$. For each of the instances $i = 1, 2, 3, *$, we set $\mu_i = C \|\Phi_i x\|_\infty$, $C = 10^{-1}$ or $C = 1$, since we noticed an improved performance of the algorithm when μ is a function of Φ_i (the scaling factor C and the function $\|\cdot\|_\infty$ are simply chosen empirically).
- from the aforementioned procedure, we obtain four different estimators for each x , namely $\hat{x}_1, \hat{x}_2, \hat{x}_3, \hat{x}_*$ and their corresponding relative errors $\|x - \hat{x}_i\|_2 / \|x\|_2$, $i = 1, 2, 3, *$.

We would like to mention at this point that, since we are interested in a comparison among star Gabor analysis operator generated by g_* and three other Gabor analysis operators –generated by state-of-the-art window vectors– we do not require a specific threshold of perfect reconstruction of x here; we only aim to show how the four previous window vectors affect implicitly the approximate success of (4), as the number of measurements increases.

4.3 Tables and Figures

The labels of all signals, along with short description and some key characteristics of the application of our framework to all signals, can be found in Table 1.

Table 1: Signals' details and summary of parameters

Labels	Samples	(L, a, b)	x_0	$\mu_i, i = 1, 2, 3, *$
Cusp	33	(33, 1, 11)	zero vector	$\ \Phi_i x\ _\infty$
Blocks	63	(63, 9, 1)	zero vector	$\ \Phi_i x\ _\infty$
Ramp	33	(33, 1, 11)	zero vector	$\ \Phi_i x\ _\infty$
Sing	45	(45, 1, 9)	zero vector	$\ \Phi_i x\ _\infty$
SI1899	22938	(20349, 19, 21)	$A^T Ax$	$10^{-1} \ \Phi_i x\ _\infty$
SI1948	27680	(27531, 19, 23)	$A^T Ax$	$10^{-1} \ \Phi_i x\ _\infty$
SI2141	42800	(41769, 21, 17)	$A^T Ax$	$10^{-1} \ \Phi_i x\ _\infty$
SX5	24167	(23205, 17, 13)	$A^T Ax$	$10^{-1} \ \Phi_i x\ _\infty$
SX224	25805	(24633, 23, 21)	$A^T Ax$	$10^{-1} \ \Phi_i x\ _\infty$
SI1716	25908	(24633, 23, 21)	$A^T Ax$	$\ \Phi_i x\ _\infty$

The resulting figures on the following pages, show the relative reconstruction error decay as the number of measurements increases. Fig. 1 demonstrates the

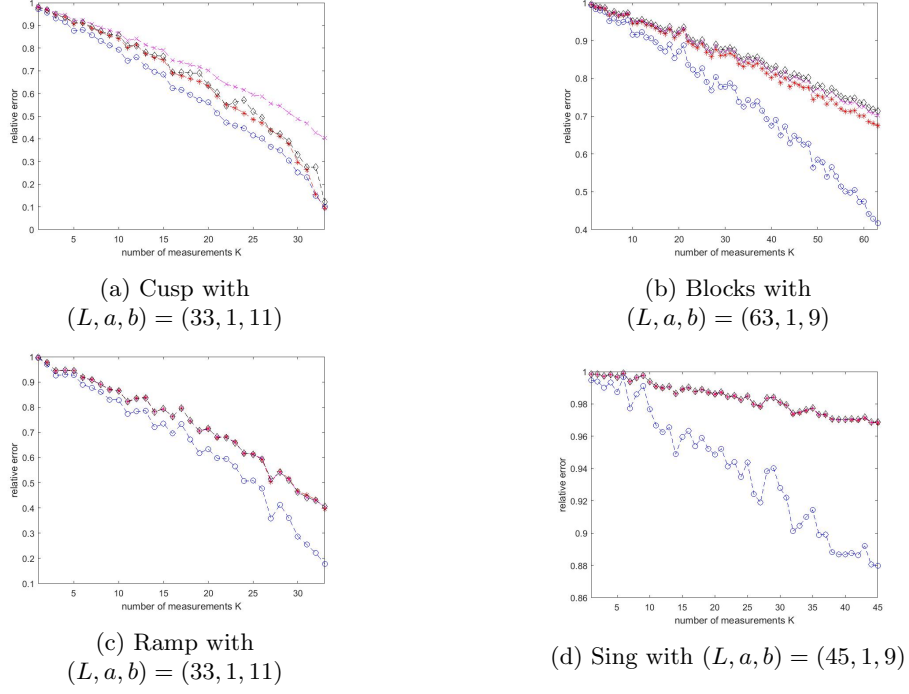


Fig. 1: Rate of approximate success for synthetic data for different parameters (L, a, b) . Red: Gaussian, magenta: Hann, black: Hamming, blue: proposed.

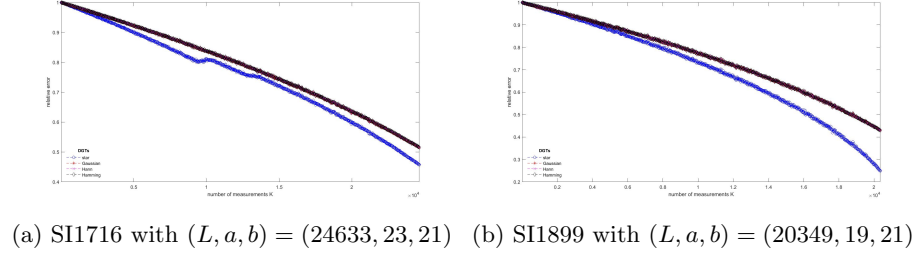
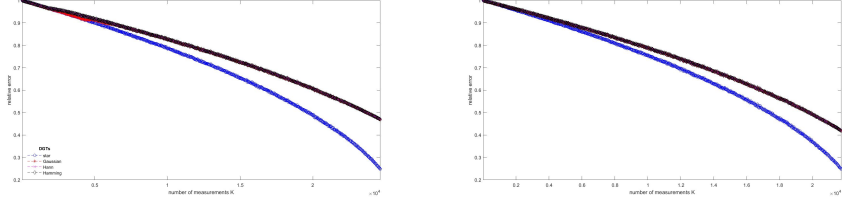


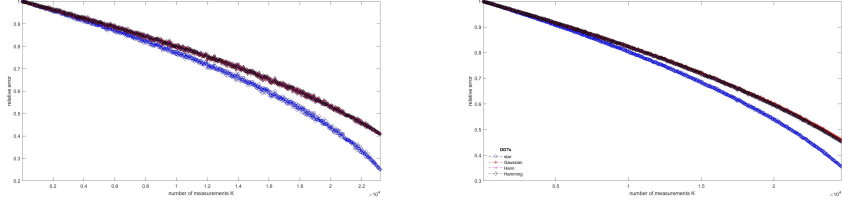
Fig. 2: Rate of approximate success for real-world signals for different parameters (L, a, b) . Red: Gaussian, magenta: Hann, black: Hamming, blue: proposed.

success rate of our proposed DGT (blue line), outperforming the rest of DGTs for the synthetic data. Similarly, for the real-world signals, Fig. 2, 3 and 4 indicate that our method (again blue line) achieves state-of-the-art performance in the first approximately 20% of the measurements and from this point on, star-DGT outperforms the rest of DGTs.



(a) SI1948 with $(L, a, b) = (24633, 21, 23)$ (b) SI2141 with $(L, a, b) = (21735, 21, 23)$

Fig. 3: Rate of approximate success for real-world signals for different parameters (L, a, b) . Red: Gaussian, magenta: Hann, black: Hamming, blue: proposed.



(a) SX5 with $(L, a, b) = (23205, 17, 13)$ (b) SX224 with $(L, a, b) = (24633, 23, 21)$

Fig. 4: Rate of approximate success for real-world signals for different parameters (L, a, b) . Red: Gaussian, magenta: Hann, black: Hamming, blue: proposed.

5 Conclusion and Future Work

In the present paper, we took advantage of a window vector to generate a spark deficient Gabor frame and introduced a novel redundant analysis operator/DGT, namely the star DGT, associated with this SDGF. We then applied the star DGT to analysis Compressed Sensing, along with three other DGTs generated by state-of-the-art window vectors in the field of Gabor Analysis. Our experiments confirm improved performance: the increased amount of linear dependencies provided by this SDGF, yields in all cases lower relative reconstruction error for both synthetic and real-world data, as the number of measurements increases. Future directions will be the extension of the present framework to largescale problems (e.g. images or videos). Additionally, it would be interesting to compare this star-DGT to other similar choices of redundant analysis operators (e.g. redundant wavelet transform, shearlets [11] etc.).

References

- [1] Emmanuel J Candès, Justin Romberg, and Terence Tao. “Robust uncertainty principles: Exact signal reconstruction from highly incomplete frequency information”. In: *IEEE Transactions on information theory* 52.2 (2006), pp. 489–509.
- [2] Lee C Potter et al. “Sparsity and compressed sensing in radar imaging”. In: *Proceedings of the IEEE* 98.6 (2010), pp. 1006–1020.
- [3] Junxin Chen et al. “Exploiting chaos-based compressed sensing and cryptographic algorithm for image encryption and compression”. In: *Optics & Laser Technology* 99 (2018), pp. 238–248.
- [4] George C Alexandropoulos and Symeon Chouvardas. “Low complexity channel estimation for millimeter wave systems with hybrid A/D antenna processing”. In: *2016 IEEE Globecom Workshops (GC Wkshps)*. IEEE. 2016, pp. 1–6.
- [5] Michael Lustig et al. “Compressed sensing MRI”. In: *IEEE signal processing magazine* 25.2 (2008), pp. 72–82.
- [6] Yan Wu, Mihaela Rosca, and Timothy Lillicrap. “Deep compressed sensing”. In: *International Conference on Machine Learning*. PMLR. 2019, pp. 6850–6860.
- [7] Pradeep Sen and Soheil Darabi. “Compressive rendering: A rendering application of compressed sensing”. In: *IEEE Transactions on Visualization and Computer Graphics* 17.4 (2010), pp. 487–499.
- [8] Simon Foucart and Holger Rauhut. “A mathematical introduction to compressive sensing”. In: *Bull. Am. Math* 54.2017 (2017), pp. 151–165.
- [9] Chen Li and Ben Adcock. “Compressed sensing with local structure: uniform recovery guarantees for the sparsity in levels class”. In: *Applied and Computational Harmonic Analysis* 46.3 (2019), pp. 453–477.
- [10] Slavche Pejowski, Venceslav Kafedziski, and Dušan Gleich. “Compressed Sensing MRI Using Discrete Nonseparable Shearlet Transform and FISTA”. In: *IEEE Signal Processing Letters* 22.10 (2015), pp. 1566–1570. DOI: 10.1109/LSP.2015.2414443.
- [11] Min Yuan et al. “Compressed sensing MRI reconstruction from highly undersampled-space data using nonsubsampling shearlet transform sparsity prior”. In: *Mathematical Problems in Engineering* 2015 (2015).
- [12] Phuong Thi Dao, Anthony Griffin, and Xue Jun Li. “Compressed Sensing of EEG with Gabor Dictionary: Effect of Time and Frequency Resolution”. In: *2018 40th Annual International Conference of the IEEE Engineering in Medicine and Biology Society (EMBC)*. 2018, pp. 3108–3111. DOI: 10.1109/EMBC.2018.8513071.
- [13] Hamza Cherkaoui et al. “Analysis vs synthesis-based regularization for combined compressed sensing and parallel MRI reconstruction at 7 tesla”. In: *2018 26th European Signal Processing Conference (EUSIPCO)*. IEEE. 2018, pp. 36–40.

- [14] Martin Genzel, Gitta Kutyniok, and Maximilian März. “ l_1 -Analysis minimization and generalized (co-) sparsity: When does recovery succeed?” In: *Applied and Computational Harmonic Analysis* 52 (2021), pp. 82–140.
- [15] Maryia Kabanava and Holger Rauhut. “Analysis l_1 -recovery with frames and Gaussian measurements”. In: *Acta Applicandae Mathematicae* 140.1 (2015), pp. 173–195.
- [16] Emmanuel J Candes et al. “Compressed sensing with coherent and redundant dictionaries”. In: *Applied and Computational Harmonic Analysis* 31.1 (2011), pp. 59–73.
- [17] Sangnam Nam et al. “The cosparsity analysis model and algorithms”. In: *Applied and Computational Harmonic Analysis* 34.1 (2013), pp. 30–56.
- [18] Maryia Kabanava and Holger Rauhut. “Cosparsity in compressed sensing”. In: *Compressed Sensing and Its Applications*. Springer, 2015, pp. 315–339.
- [19] Felix Krahmer, Christian Kruschel, and Michael Sandbichler. “Total variation minimization in compressed sensing”. In: *Compressed Sensing and its Applications*. Springer, 2017, pp. 333–358.
- [20] Leonid I Rudin, Stanley Osher, and Emad Fatemi. “Nonlinear total variation based noise removal algorithms”. In: *Physica D: nonlinear phenomena* 60.1-4 (1992), pp. 259–268.
- [21] Thomas Blumensath and Mike E Davies. “Sampling theorems for signals from the union of finite-dimensional linear subspaces”. In: *IEEE Transactions on Information Theory* 55.4 (2009), pp. 1872–1882.
- [22] Gerhard Zauner. “Quantum Designs”. PhD thesis. University of Vienna Vienna, 1999.
- [23] Götz E Pfander and Holger Rauhut. “Sparsity in time-frequency representations”. In: *Journal of Fourier Analysis and Applications* 16.2 (2010), pp. 233–260.
- [24] Shristi Rajbanshi et al. “Random Gabor multipliers for compressive sensing: a simulation study”. In: *2019 27th European Signal Processing Conference (EUSIPCO)*. IEEE, 2019, pp. 1–5.
- [25] Julien Richy et al. “Blood velocity estimation using compressive sensing”. In: *IEEE transactions on medical imaging* 32.11 (2013), pp. 1979–1988.
- [26] Stephen R Becker, Emmanuel J Candès, and Michael C Grant. “Templates for convex cone problems with applications to sparse signal recovery”. In: *Mathematical programming computation* 3.3 (2011), p. 165.
- [27] P. L. Søndergaard, P. C. Hansen, and O. Christensen. “Finite discrete Gabor analysis”. PhD thesis. Technical University of Denmark, 2007.
- [28] R.-D. Malikiosis. “A note on Gabor frames in finite dimensions”. In: *Applied and Computational Harmonic Analysis* 38.2 (2015), pp. 318–330.
- [29] Stephan Paukner. “Foundations of Gabor analysis for image processing”. MA thesis. University of Vienna, 2007.
- [30] H. B. Dang et al. “Linear dependencies in Weyl–Heisenberg orbits”. In: *Quantum Information Processing* 12.11 (2013), pp. 3449–3475.
- [31] R.-D. Malikiosis. “Spark deficient Gabor frames”. In: *Pacific Journal of Mathematics* 294.1 (2018), pp. 159–180.

- [32] Jonathan B Buckheit and David L Donoho. “Wavelab and reproducible research”. In: *Wavelets and statistics*. Springer, 1995, pp. 55–81.
- [33] John S Garofolo et al. “DARPA TIMIT acoustic-phonetic continous speech corpus CD-ROM. NIST speech disc 1-1.1”. In: *NASA STI/Recon technical report n 93* (1993), p. 27403.
- [34] Thomas E Booth. “Power iteration method for the several largest eigenvalues and eigenfunctions”. In: *Nuclear science and engineering* 154.1 (2006), pp. 48–62.
- [35] Zdenek Pruša et al. “LTFAT: A Matlab/Octave toolbox for sound processing”. In: *Proc. 10th International Symposium on Computer Music Multidisciplinary Research (CMMR)*. 2013, pp. 299–314.